energies

Article

Analysis of the Impact of a Photovoltaic Farm on Selected Parameters of Power Quality in a Medium-Voltage Power Grid

Grzegorz Hołdyński [1], Zbigniew Skibko [1,*], Andrzej Firlit [2] and Wojciech Walendziuk [1]

[1] Faculty of Electrical Engineering, Bialystok University of Technology, Wiejska 45D, 15-351 Bialystok, Poland; g.holdynski@pb.edu.pl (G.H.); w.walendziuk@pb.edu.pl (W.W.)
[2] Faculty of Electrical Engineering, Automatics, Computer Science and Biomedical Engineering, AGH University of Science and Technology, al. Adama Mickiewicza 30, 30-059 Krakow, Poland; afirlit@agh.edu.pl
* Correspondence: z.skibko@pb.edu.pl

Abstract: Over the last few years, a dynamic increase in the installed capacity of distributed energy sources has been observed, with the largest share being photovoltaic sources. The power grid is a system of connected vessels, and changing the structure of electricity production has a specific impact on the operation of this network, which makes it necessary to study the impact of the sources on the power system. The current and projected increase in the number of connected installations will make the issues of interaction and cooperation of distributed sources with the network extremely important. The article presents an analysis of the impact of a photovoltaic farm on selected parameters of the quality of electricity supply. This analysis was made on the basis of simulation results in a computer program and measurement tests carried out on a real photovoltaic farm with a capacity of 1.8 MW connected to the medium voltage power grid. The impact of the farm-generated power on the values of fundamental indicators of the quality of electricity supply, such as voltage deviations, voltage asymmetry factors, and voltage distortions factors, is presented. These relationships were determined based on the correlation and regression analysis of individual electrical quantities.

Keywords: distributed energy source; photovoltaic farm; power quality; medium voltage power grid

check for updates

Citation: Hołdyński, G.; Skibko, Z.; Firlit, A.; Walendziuk, W. Analysis of the Impact of a Photovoltaic Farm on Selected Parameters of Power Quality in a Medium-Voltage Power Grid. *Energies* **2024**, *17*, 623. https://doi.org/10.3390/en17030623

Received: 13 January 2024
Revised: 23 January 2024
Accepted: 25 January 2024
Published: 27 January 2024

Copyright: © 2024 by the authors. Licensee MDPI, Basel, Switzerland. This article is an open access article distributed under the terms and conditions of the Creative Commons Attribution (CC BY) license (https://creativecommons.org/licenses/by/4.0/).

1. Introduction

The energy from photovoltaic installations is considered one of the most promising renewable sources [1]. However, the variable nature of production in photovoltaic installations, similar to wind power plants, significantly affects the quality of the energy transmitted in power grids [2,3]. The quality of electricity supply is a set of parameters that describe the features of the process of supplying energy to the user under normal operating conditions [4]. In Poland, legal regulations regarding the quality of supply voltage are defined mainly as:

- EN 50,160 parameters of supply voltage in public distribution networks [5];
- Regulation of the Government Minister of Climate and Environment of 22 March 2023 on detailed conditions for the operation of the power system [6].

1.1. Changes in the Value of the Supply Voltage

A change in the supply voltage occurs when the voltage increases or decreases, which is usually caused by a change in the load on the power grid or a change in the amount of power generated by the sources. There are two types of changes in voltage values: slow changes, called voltage deviation, which occur at a rate less than 0.02 U_n per second, and fast changes, called voltage fluctuations, which occur at a rate greater than this limit [7,8]. For medium voltage power networks, the voltage deviation should not exceed 10% of the rated voltage concerning 95% of the weekly working time [5,6]. Most devices are sensitive to voltage fluctuations, especially voltage dips [9,10]. Currently, the applicable regulations require that the voltage fluctuations caused by sources at their point of connection (PCC) do not exceed 3% of the rated network voltage [11–13]. Various methods of reducing voltage fluctuations from photovoltaic installations by reducing fluctuations in photovoltaic output power are described in the literature. The use of a Kalman filter effectively smooths the power, minimizing stress in the converter [14]. Battery energy storage can also be used to limit voltage changes caused by changes in the power generated in photovoltaics [15–18].

1.2. Voltage Asymmetry

The condition of asymmetry is characterized by the fact that there are unequal voltage values in each phase or values of angles between successive voltages. Asymmetric voltage systems can be decomposed into symmetric components using the Fortescue transform [19]:

$$\begin{aligned} \underline{U}_0 &= \tfrac{1}{3}\cdot(\underline{U}_{L1} + \underline{U}_{L2} + \underline{U}_{L3}) \\ \underline{U}_1 &= \tfrac{1}{3}\cdot(\underline{U}_{L1} + a\cdot\underline{U}_{L2} + a^2\cdot\underline{U}_{L3}) \\ \underline{U}_2 &= \tfrac{1}{3}\cdot(\underline{U}_{L1} + a^2\cdot\underline{U}_{L2} + a\cdot\underline{U}_{L3}) \end{aligned} \tag{1}$$

or in the matrix form:

$$\begin{bmatrix} \underline{U}_0 \\ \underline{U}_1 \\ \underline{U}_2 \end{bmatrix} = \frac{1}{3}\begin{bmatrix} 1 & 1 & 1 \\ 1 & a & a^2 \\ 1 & a^2 & a \end{bmatrix}\begin{bmatrix} \underline{U}_{L1} \\ \underline{U}_{L2} \\ \underline{U}_{L3} \end{bmatrix} \tag{2}$$

where $\underline{U}_0$, $\underline{U}_1$, $\underline{U}_2$—complex values of the symmetric components of the zero, positive, and negative sequences of voltage, $\underline{U}_{L1}$, $\underline{U}_{L2}$, $\underline{U}_{L3}$—complex values of phase voltages, and a—rotation operator described using the equation:

$$a = e^{j\frac{2\pi}{3}} \tag{3}$$

Two asymmetry coefficients describe the level of voltage asymmetry in power systems. One of them is the opposite asymmetry factor $\alpha U2\%$, which describes the inequality of the values or angles of the interfacial voltages [20,21]:

$$\alpha_{U2\%} = \left|\frac{\underline{U}_2}{\underline{U}_1}\right|\cdot 100\% \tag{4}$$

Whereas the other one, which defines the inequality of the values or angles of the phase voltages, is described using the zero asymmetry factor $\alpha U0\%$ [19]:

$$\alpha_{U0\%} = \left|\frac{\underline{U}_0}{\underline{U}_1}\right|\cdot 100\% \tag{5}$$

Unequal voltage drops in individual phases caused by load asymmetry (uneven distribution of single-phase receivers among consumers) are the leading cause of voltage asymmetry in power networks [11,22]. In the case of medium-voltage networks, additional unevenness of earth capacitances may occur, mainly in the overhead lines and incorrect tuning of the compensating choke, in networks operating with a neutral point grounded using a Petersen coil, leading to resonance [23,24]. Renewable energy sources may serve as sources of voltage asymmetry: photovoltaic power plants [22,25,26], wind farms [4], agricultural biogas plants [27,28], electric car charging stations [29–31], and energy storage facilities [32,33].

The values of the negative-sequence voltage asymmetry factor in medium voltage power systems, in accordance with applicable guidelines, should not exceed 2% for 95% of the week [5,6]. The IEEE Standard 1547-2014 [34] requires that voltage asymmetry does not exceed 3%, while Romanian regulations have imposed a maximum $\alpha U2\%$ of 1% on photovoltaic and wind power plants [35].

1.3. Voltage Waveform Distortion

The total harmonic distortion factor (*THD*) is one of the most common indicators of voltage distortion used in practice [36]. It determines the percentage ratio of the *RMS* value of higher harmonics to the *RMS* value of the fundamental harmonic, according to the relation [27,37]:

$$THD_U = \frac{\sqrt{\sum_{h=2}^{h_{gr}} U_h^2}}{U_1} \cdot 100\% \quad (6)$$

where U_h is the *RMS* value of the voltage of the h-th harmonic, U_1 is the *RMS* value of the voltage of the first harmonic, h is the order of the harmonic, and h_{gr} is the limiting order of the harmonic for which the factor is calculated, for example, 40 or 50 [5,6].

The voltage distortion is mainly affected by nonlinear loads and sources, among which power electronic devices (rectifiers, inverters, etc.) predominate [36]. The occurrence of higher voltage harmonics in power grids causes effects related to the flow of distorted currents through the components of power systems, as well as the effects caused by supplying equipment with voltage distorted from the sinusoidal waveform [38]. Higher harmonic currents flowing through the elements of power networks (lines and transformers) cause additional power losses caused by an increase in the RMS value of current and wire resistance caused by the skin effect and the proximity effect, in the case of transmission lines, or an increase in dissipation and eddy current losses, in the case of transformers [27,39–41]. According to the currently applicable regulations [5,6], the voltage distortion factor THD_U value in medium voltage networks cannot exceed 8%. According to the requirements of IEEE 519-2014, IEEE 1547-2014, and IEC 61,727 [42–44], the THD_U factor should not exceed, at the point of connection of the power plant, a value of 5%. Standards in some countries, including Brazil's ABNT 16,149 [34] and Malaysia's Technical Regulations [45], also require a THD_U of less than 5% at the point of connection.

The issue of the impact of photovoltaic power plants on the quality of energy in power grids is not new. Unfortunately, most of the available articles concern the impact of power plants on the low-voltage network. According to research conducted by Kopicka et al. [46], small photovoltaic power plants cause an increase in the voltage distortion coefficient and significantly affect the voltage value in the low-voltage network. Similarly, in [47], it was shown that power generation in a photovoltaic installation increases the voltage distortion occurring in the network (regardless of the voltage level). Analogous conclusions were drawn by Amirullah Penangsang and Soeprijanto for industrial and residential networks [48]. Fluctuations of the solar energy source in the power supply to the load cause overvoltage or blackouts, which can negatively influence sensitive loads [47].

Photovoltaic installations can reduce transmission line overloads and limit the occurrence of peak power values [49], which cause voltage changes, bidirectional power flow, and problems with protection settings [50]. Shetwi et al. [22] presented possibilities for reducing interference occurring in medium-voltage power grids via photovoltaic inverters. Mehrdad and Tohid described the requirements of grid codes regarding the need to generate reactive power in photovoltaic power plants. However, no research has been undertaken on the impact of the operation of the power plant itself on the network voltage. According to research conducted by Elshahed [51], turning off or turning on a photovoltaic installation leads to voltage fluctuations significantly exceeding the permissible values. In order to reduce the impact, the author suggested installing a 150 Ω resistor at the connection point. Saidi et al. [52] and Till et al. [53] demonstrated the impact of photovoltaic power plants on the stability of the power system, mainly by introducing voltage fluctuations. The need for an in-depth analysis of the impact of renewable electricity sources on the power grid was also indicated by Hossain et al. in their publication [54]. Therefore, the authors attempted to fill this research gap.

In this article, the authors attempted to determine the impact of power generated in a photovoltaic power plant on selected parameters of the electricity quality by performing simulation and field tests. In the first part of the research, a computer model of the medium-voltage power grid was made, to which a 1.8 MW photovoltaic power plant was connected. Parameters characterizing individual elements included in the analyzed system are given. The rest of the study presents the results of simulation studies. The second stage of the research was to measure the impact of a real photovoltaic power plant on selected electricity quality parameters, the results of which are presented later in the study. The research ends with a discussion of the research results of other authors and conclusions.

2. Characteristics of the Tested Object and Measuring Equipment

The research covered a photovoltaic farm located in eastern Poland with a 1.8 MW capacity and connected to the medium voltage power grid. The farm consists of monocrystalline photovoltaic modules with a capacity of 575 W and inverters with a capacity of 225 kW (Table 1). It is connected to the network through a transformer with a rated power of 2000 kVA and rated voltages of 15.75/0.8 kV (Table 2). The farm was connected to a medium-voltage overhead line (line tap) with aluminum conductor steel-reinforced (ACSR) conductors with a cross-section of 70 mm^2 (Table 3). The connection point is located 5.4 km from the main power supply (MPS) station.

Table 1. Parameters of the Sungrow SG225HX inverter.

Parameter	Value
AC output power	225 kW
Maximum AC output current	180.5 A
Rated AC voltage	800 V
AC voltage range	680–880 V
Rated grid frequency	50 Hz
Total harmonic distortion factor	*THD* < 3%
DC component of current	<0.5% In
Power factor	0.8 inductive–0.8 capacitive
Maximum efficiency	99.00%
Maximum PV input voltage	1500 V
MPP voltage range	500–1500 V
Number of independent MPP inputs	12

Table 2. Parameters of the transformer installed in the photovoltaic farm.

Parameter	Value
Rated power	2000 kVA
Maximal voltage rating	15 kV
Minimum voltage rating	0.8 kV
Connection group	Dy11
Rated frequency	50 Hz
Rated current of the medium voltage side	630 A
Short circuit voltage	7.5%
Load losses	12.8 kW
Idle losses	4.8 kW

Table 3. Parameters of the overhead line with ACSR 70 cables.

Parameter	Value
Unit resistance for a positive-sequence component	R_1 0.44 Ω/km
Unit reactance for a positive-sequence component	X_1 0.391 Ω/km
Unit capacity for a positive-sequence component	C_1 0.009 µF/km
Specific resistance for a zero-sequence component	R_0 0.588 Ω/km
Unit reactance for a zero-sequence component	X_0 1.521 Ω/km
Long-term current-carrying capacity	290 A

The research on the impact of the photovoltaic farm was carried out in two stages. Firstly, a mathematical model of a fragment of the power grid with a connected photovoltaic installation was created in the Neplan computer program (Figure 1). The model parameters were selected in such a way that they were as close to the parameters of the real network in which the measurement tests were carried out as possible. These values were taken from the catalog data obtained from the distribution system operator and the operator of the analyzed photovoltaic farm.

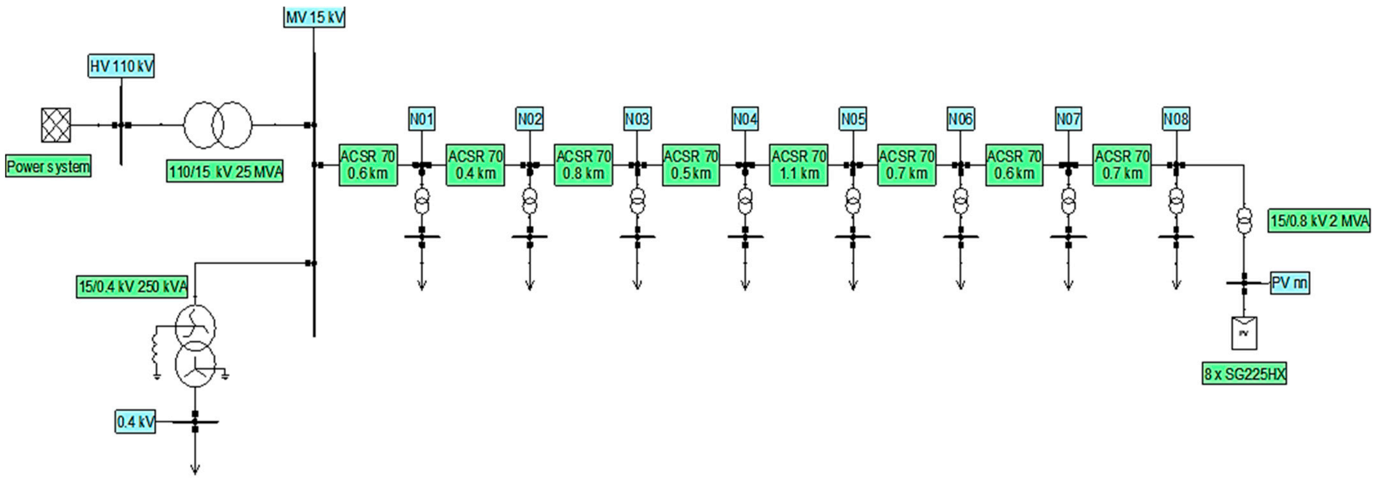

Figure 1. The computer model of a fragment of the power network made in the Neplan program used for further simulation.

When creating a model of a fragment of the power network, it was assumed, analogously to the tested real network, that it was powered by the power system at a level of 110 kV at the connection point with a short-circuit power of 1100 MVA. A 25 MVA transformer was installed in the HV/MV power supply station. In the computer model, a grounding transformer with a Znyn11 connection system with a power of 0.25 MVA and a quenching choke (Petersen coil) with an impedance of 430 Ω was used to ground the neutral point of the MV network. The degree of detuning of the earth fault compensation was assumed to be 10%, of an inductive nature (overcompensation). Similarly to the case of the real network, the model assumes the same layout of a photovoltaic farm with a capacity of 1.8 MW connected to the MV overhead line at a distance of 5.4 km from the power supply station via a transformer with a rated power of 2000 kVA. In the overhead line, bare ACSR-type wires with a cross-section of 70 mm^2 were modeled in a flat arrangement at a distance of 1.85 m. Eight 15/0.4 kV power stations with transformers with a rated power of 0.1 MVA were connected to the overhead line. All receiving stations were loaded symmetrically with the power of 90 kW at a power factor cosφ = 0.95 of an inductive nature. During the simulation, a symmetrical input voltage at the power supply point (HV 110 kV) was assumed with a value of 103% of the rated voltage (113 kV). The distortion of the supply voltage was assumed, as in the tested real network, at the level of THD_U = 10% with a spectrum with dominant harmonics of orders 5 and 7. The distortion of the currents consumed by consumers on the low voltage side of these stations was assumed at the level of a THD_I = 10% spectrum with dominant harmonics of orders 3, 5, and 7. In the case of the wind farm, it was assumed, as for the measurement data, that it generates a symmetrical voltage with a distortion of THD_U = 1.2% and a spectrum with dominant harmonics of orders 3, 5, and 7.

During the simulation, subsequent calculations were made, increasing the generated power from 0 to 1.8 MW in steps of 0.15 MW and obtaining the values of basic voltage parameters for all nodes of the analyzed part of the power grid. In the Neplan program, the Newton–Raphson algorithm is used to calculate power flows and voltage levels.

The second stage of the research was the verification of the results obtained from simulation calculations by performing field tests of changes in the analyzed electricity quality parameters in a real photovoltaic farm. The research on the analyzed photovoltaic farm is based on measurements and recordings carried out for one week, from 21 to 28 September 2023. The values of the basic electrical quantities, such as voltage, current, active and reactive power, and power factors, were collected. Moreover, an appropriate set of indicators allowing for the analysis and assessment of the quality of energy supply in accordance with applicable regulations, including voltage and current asymmetry factors, light flicker factors, and harmonic content factors, were taken into account. The data logging took place with a 10 min period of aggregation and recording of measured values.

The measurement equipment was connected to the power grid at the farm connection point at a medium voltage (15 kV) using an indirect current and voltage measurement through a set of transformers. A portable power quality analyzer MAVOWATT 240 from GOSSEN METRAWATT was used to record electrical quantities, with a calibration certificate issued by the Drantez Laboratory. The analyzer is intended for long-term measurements and recording of operating parameters of single-phase or three-phase power networks in accordance with applicable international standards.. It allows for measurements in installations with categories CAT III and CAT IV. The device played the role of a programmable device with features for measuring, calculating, and storing the operating parameters of power networks. Moreover, it allowed measurements and recording of electrical quantities in steady states and event-disturbance conditions, recording transient states up to 10,000 cycles with a 512 samples/cycle frequency. The measurement results were saved at selected time intervals with the minimum measurement aggregation time of 10 ms, which equaled ½ period, to the device's internal memory and then transferred to a PC for further analysis.

During the analysis of the field research results, a correlation analysis was performed between selected values. Pearson's linear correlation coefficient, which is the most frequently used measure of the strength of the relationship between two measurable features, x and y, was chosen as a measure of this correlation. The value of the coefficient can be expressed using the formula:

$$r = \frac{\sum_{i=1}^{n}(x_i - \overline{x})(y_i - \overline{y})}{\sqrt{\sum_{i=1}^{n}(x_i - \overline{x})^2 \sum_{i=1}^{n}(y_i - \overline{y})^2}} \tag{7}$$

where x_i—i-th observation of the independent (explanatory) variable, y_i—i-th observation of the dependent (explained) variable, n—sample size, and $\overline{x}$, $\overline{y}$—average values of individual variables determined from the relationship:

$$\overline{x} = \frac{1}{n}\sum_{i=1}^{n} x_i \quad \overline{y} = \frac{1}{n}\sum_{i=1}^{n} y_i \tag{8}$$

Pearson's linear correlation coefficient tells about the strength and direction of the relationship between variables. It takes values in the range $[-1; 1]$. The closer it is to "0", the weaker the relationship. The closer to "1" (or "-1"), the stronger the relationship. The sign of the correlation coefficient indicates the direction of the relationship: "+" means a positive relationship, i.e., an increase (decrease) in the value of one feature causes an increase (decrease) in the value of the other (directly proportional relationship). The "$-$" sign indicates a negative direction, i.e., an increase (decrease) in the value of a feature causes a decrease (increase) in the value of the other (inversely proportional relationship). The strength of the relationship is considered to be strong for r in the range of 0.7–0.9 or very strong for r = 0.9 or more.

An issue directly related to the Pearson correlation analysis r is the coefficient of determination R^2. Mathematically, it is the value of the square of the Pearson correlation coefficient. The R^2 value tells us what percentage of the variability of the dependent variable is explained by the variability of the independent variable. The R^2 coefficient can range from 0 to 1. If it equals 0, it means that the model explains 0% of the variability of the examined variable, i.e., it does not help to explain the examined variable. If the R^2 value is 1, the model explains 100% of the variables under study, i.e., they are perfectly related. In practice, however, there are usually various disturbing variables that influence the value of the dependent variable.

3. Analysis of Results from Simulation Calculations

Figure 2 shows the analytically determined relationship between the voltage at the connection point of a photovoltaic power plant and the power generated in the photovoltaic installation.

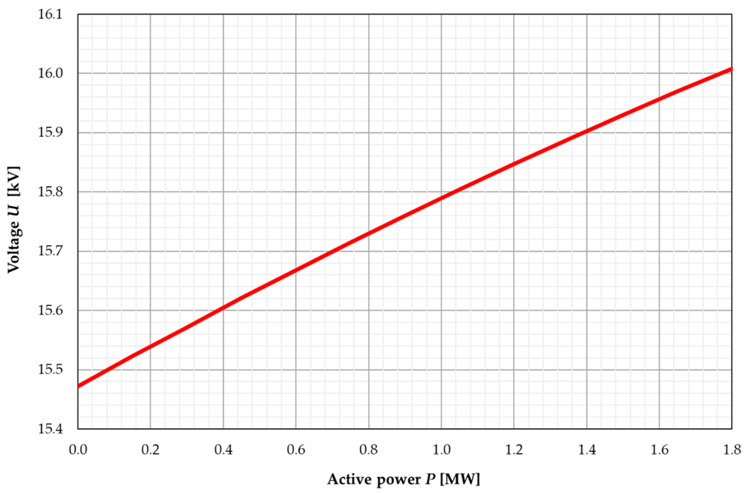

Figure 2. Dependence of voltage on the power generated at the connection point of the tested photovoltaic farm.

As could be expected, with the increase in power generated at the source, there was a rectilinear increase in the voltage value at the connection point, which, at maximum power, reached more than 106% of the rated network voltage.

Another parameter analyzed was the voltage asymmetry factor [19]. Figure 3 shows the relationship between the negative-sequence voltage asymmetry factor (k_{U2}) and the power generated in a photovoltaic installation, which was determined using computer simulation. Similarly, in Figure 4, the zero-sequence voltage asymmetry factor (k_{U0}) variation curve is shown.

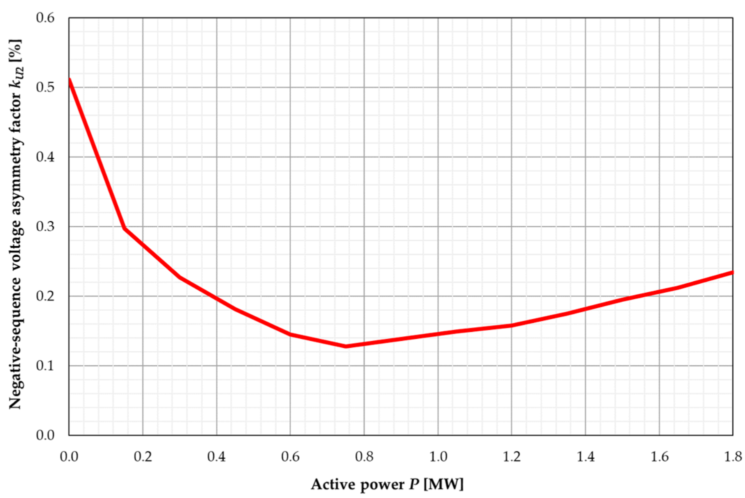

Figure 3. Dependence of the negative-sequence voltage asymmetry factor k_{U2} on the active power P generated at the connection point of the tested photovoltaic farm.

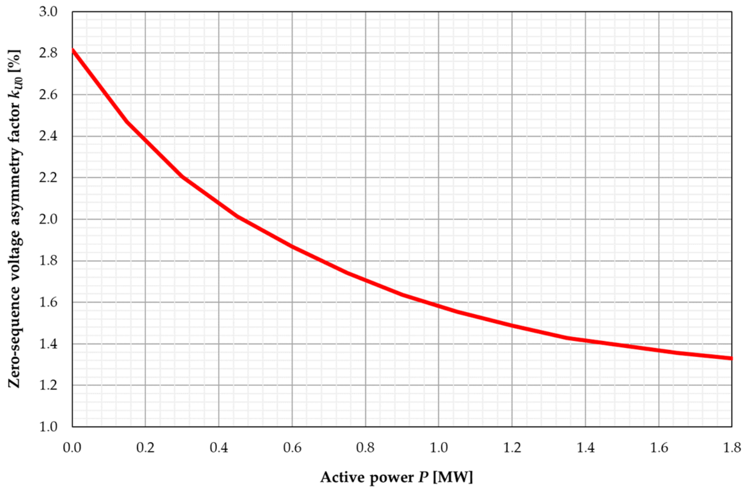

Figure 4. Dependence of the zero-sequence voltage asymmetry factor k_{U0} on the active power P generated at the connection point of the tested photovoltaic farm.

In both analyzed cases, the voltage asymmetry factors have the highest value when there is no generation in the photovoltaic installation. Both determined curves are also not rectilinear. However, in the case of the variation of the negative-sequence voltage asymmetry factor (Figure 3), an apparent saddle curve is visible, and the lowest value of this factor occurs for 45% of the rated power of the power plant. Within the range from 45% to 100% of the rated power, there is a noticeable increase in the factor value along with increasing energy production, and this change is approximately 200%. When the generated power changed from 0 to 45%, the value of the k_{U2} factor decreased by more than four times. In the case of the zero-sequence voltage asymmetry factor (Figure 4), the decrease in the factor value is visible in the entire range of generated power and amounts to approximately 210%.

The last parameter analyzed in the research was the voltage distortion factor THD_U, the variability of which, as a function of the power generated in the photovoltaic power plant, is shown in Figure 5. In this case, a decrease in the value of the THD_U factor was also observed with an increase in active power, but this time, it was a relationship rectilinear. The calculations show that power generation in a photovoltaic installation, in the analyzed case, may reduce the value of the voltage distortion factor by up to nearly 29%.

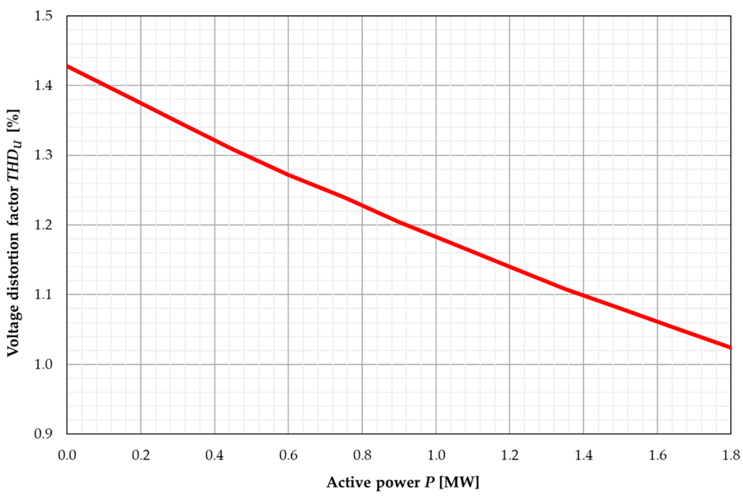

Figure 5. Dependence of the voltage distortion factor THD_U on the active power P generated at the connection point of the tested photovoltaic farm.

4. Field Test Results and Measurement Data Analysis

Figure 6 shows the recorded course of variability of the active power of the tested photovoltaic farm. The profile of the recorded curves shows that during the measurements, there were two sunny days and one day with a cloudy sky. It is worth mentioning that the power generation was recorded as less than half that of a sunny day. The remaining days were partly cloudy.

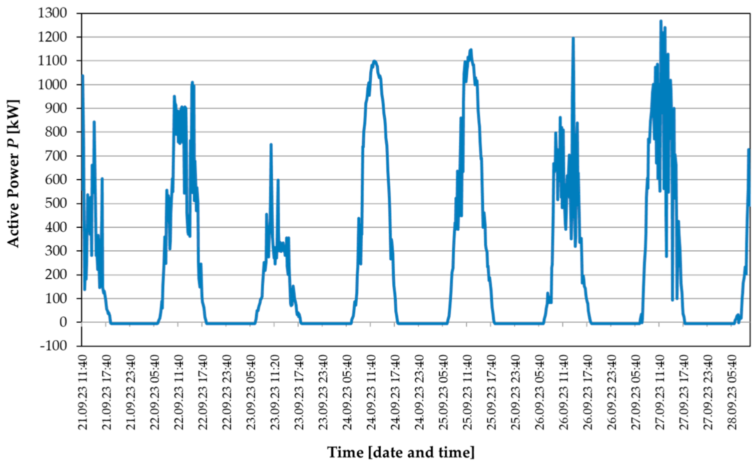

Figure 6. Recorded waveform of the variability of three-phase active power generated by the tested photovoltaic farm.

Figure 7 shows the recorded waveforms of 10 min RMS values of line-to-line voltages. Analyzing the voltage waveform recorded at the connection point of the tested photovoltaic farm, the daily variability of the voltage value in the network is clearly visible. It is higher during the day, which may be due to the work of the sources. There is also variability of the voltage value in individual hours, which is not correlated with changes in the power generated by the farm. These changes are most likely to result from the changes in the load of devices connected at other points of the medium voltage line to which the analyzed energy source is connected or deep in the network.

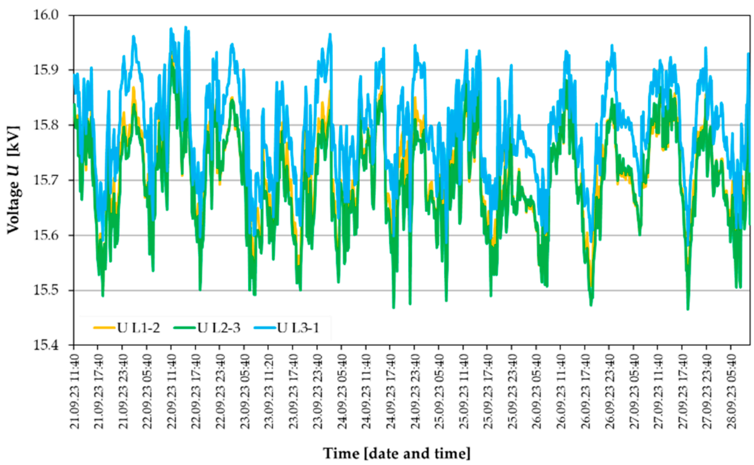

Figure 7. The course of variability of 10 min RMS values of line-to-line voltages recorded in the tested photovoltaic farm.

Figure 7 shows that the voltage variations occurring in individual phases (recorded curves) do not coincide, which may indicate voltage asymmetry. In order to verify whether the recorded changes in voltage values are within the limits permitted by regulations, the waveforms of the variability of voltage deviation from the rated value are presented in

Figure 8. The recorded waveforms show that the voltage deviation ΔU at the connection point of the analyzed photovoltaic farm ranges from 3.15% to 6.52% of the rated voltage. Voltage deviations are significantly lower than the permissible 10%.

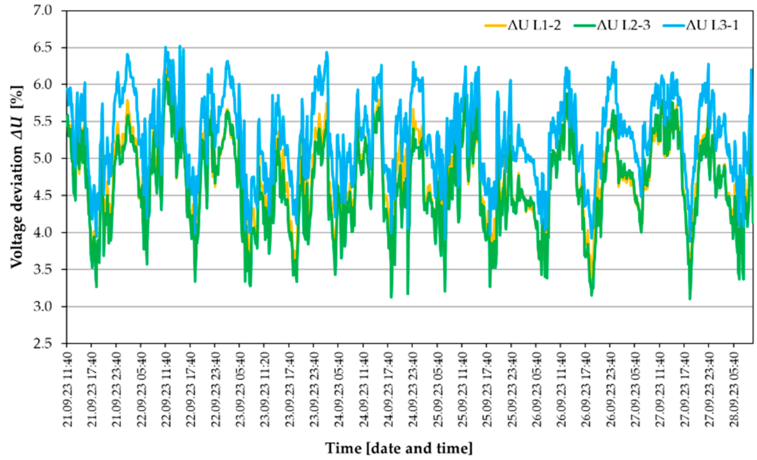

Figure 8. Voltage deviation ΔU variability recorded in the tested photovoltaic farm.

In order to check the impact of the power generated in the photovoltaic farm on the voltage at the point of connection to the grid, a correlation and regression analysis of these two indicators were performed (Figure 9). In all cases, the analysis of the interdependence of the phenomena was carried out only for the cases of power generation by the analyzed photovoltaic farm. Measurement data for cases of no generation, e.g., at night, were removed from the analysis. In this case, the determination coefficient R^2 equals 0.4911, while the Pearson correlation coefficient is 0.7, indicating a clear medium-strong positive relationship. As expected, as the power generated in the tested photovoltaic farm increases, the voltage in the power grid also increases. As it can be observable, the regression analysis showed a rectilinear relationship, which can be described by the equation shown in Figure 9.

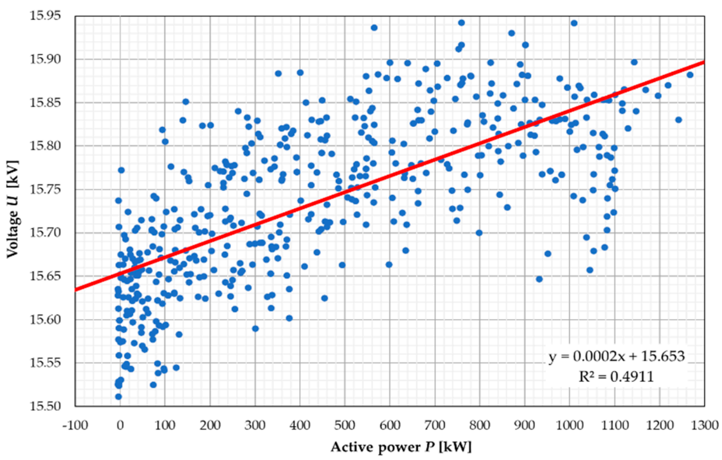

Figure 9. Dependence of line-to-line voltage on the power generated at the connection point of the tested photovoltaic farm.

As mentioned earlier, the recorded voltage waveforms indicate the occurrence of voltage asymmetry at the analyzed point in the power grid. To determine whether its value is within the range permitted by regulations, Figure 10 shows the course of the variability of 10 min voltage asymmetry factor values for the negative-sequence sequence component (k_{U2}) recorded at the farm connection point.

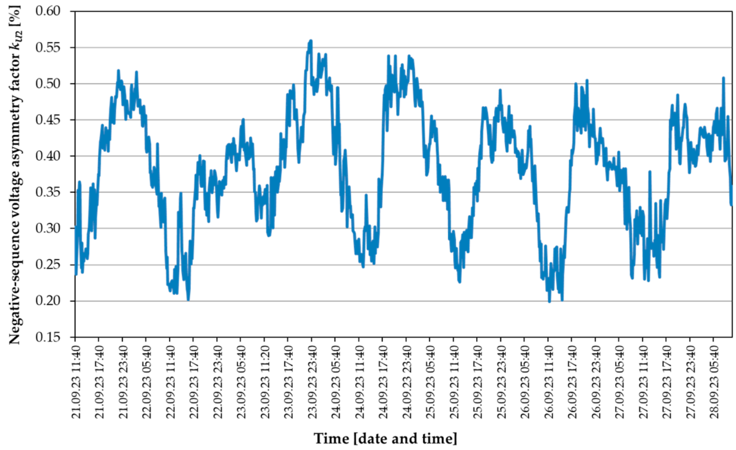

Figure 10. The course of the variability of the voltage asymmetry factor k_{U2} for the negative-sequence component recorded at the connection point of the tested photovoltaic farm.

The values in Figure 10 show that the negative-sequence voltage asymmetry factor (k_{U2}) varies from 0.2% to 0.56% during the recording period. Therefore, it is significantly lower than the permissible value of 2% specified in the regulations. Analyzing the recorded curve, the daily variability of voltage asymmetry is visible. To check whether it is caused by the operation of the farm, the relationship between the values of the negative-sequence voltage asymmetry factor and the generated active power is presented in Figure 11. The value of the determination coefficient R^2 in this case is 0.6493, while the Pearson correlation coefficient r is 0.8058, which indicates a clear (medium-strong) negative relationship.

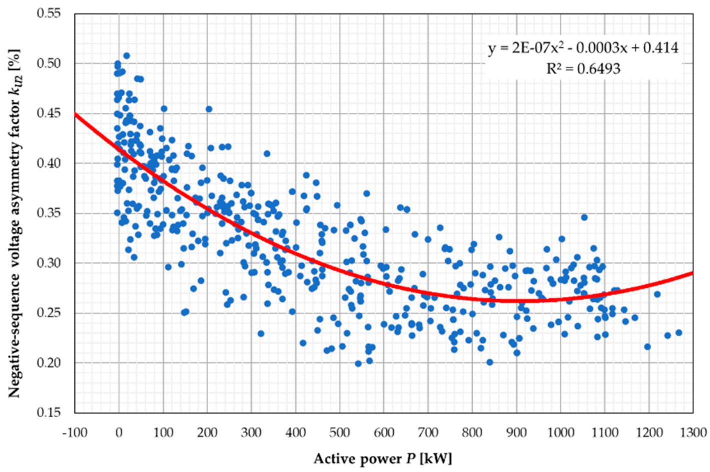

Figure 11. Dependence of the voltage asymmetry factor k_{U2} for the sequence component opposite to the active power P generated at the connection point of the tested photovoltaic farm.

The distribution of values presented in Figure 11 clearly shows that this is not a rectilinear relationship. As the active power generated by the farm increases, the value of the negative-sequence voltage asymmetry factor k_{U2} decreases, but this only happens up to approximately 50% of the installed power. The higher active powers generated by the source no longer significantly affect the value of voltage asymmetry k_{U2} and even cause its increase.

The recorded values of the voltage asymmetry factor for the zero-sequence component are shown in Figure 12. The values of the zero-sequence voltage asymmetry factor k_{U0} on the active power P generated are shown in Figure 13. There is also a clear decrease in this factor value with the increase in power generated in the power plant. In this case, an approximately rectilinear relationship can be observed. The value of the determination coefficient R^2 is 0.6829, while the Pearson correlation coefficient is r = 0.8264, which indicates a clear medium-strong negative relationship.

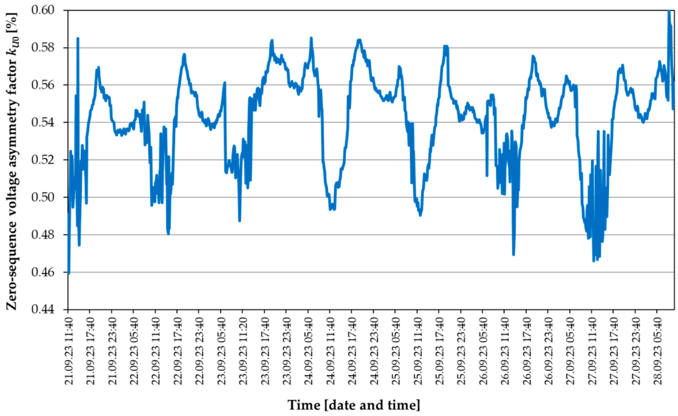

Figure 12. The course of the variability of the zero-sequence voltage asymmetry factor k_{U0} recorded at the connection point of the tested photovoltaic farm.

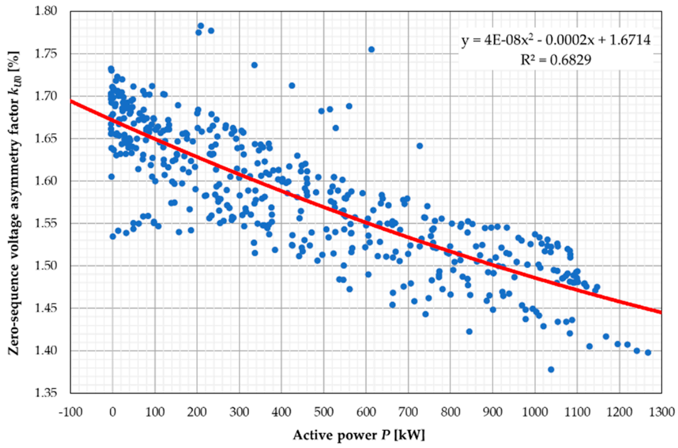

Figure 13. Dependence of the zero-sequence voltage asymmetry factor k_{U0} on the active power P generated at the connection point of the tested photovoltaic farm.

Another parameter describing the quality of electricity supply recorded at the connection point of the tested photovoltaic farm was the voltage distortion factor THD_U. Figure 14 shows the waveforms of 10 min THD_U values for the voltages in individual phases.

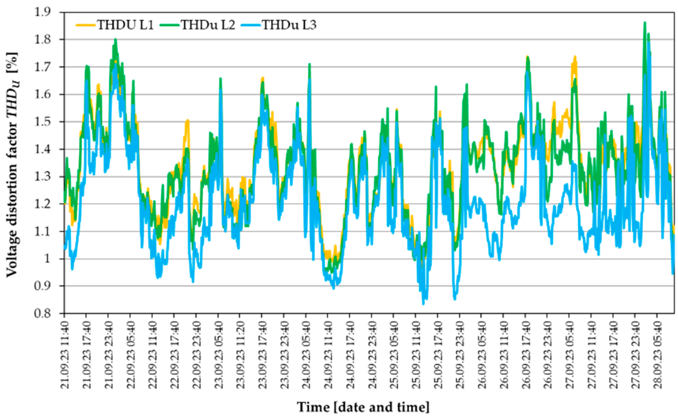

Figure 14. The course of variation of the voltage distortion factor THD_U for the voltages in individual phases recorded at the connection point of the tested photovoltaic farm.

The waveforms presented in Figure 14 show that the values of the voltage distortion factor THD_U recorded at the connection point of the tested farm vary from 0.82% to 1.86%. Therefore, they are much lower than the regulatory requirement of 8% for medium voltages. When analyzing the course of variability of the THD_U factor, unlike the previous indicators, no clear daily variability of its value was recorded.

To see how generating the active power by the farm affects the value of the voltage distortion factor THD_U, as in previous cases, a correlation and regression analysis of the two quantities was performed, which is shown in Figure 15. The value of the coefficient of determination R^2 in this case is 0.4903, while the Pearson correlation coefficient r is 0.7, indicating a clear medium-strong negative relationship.

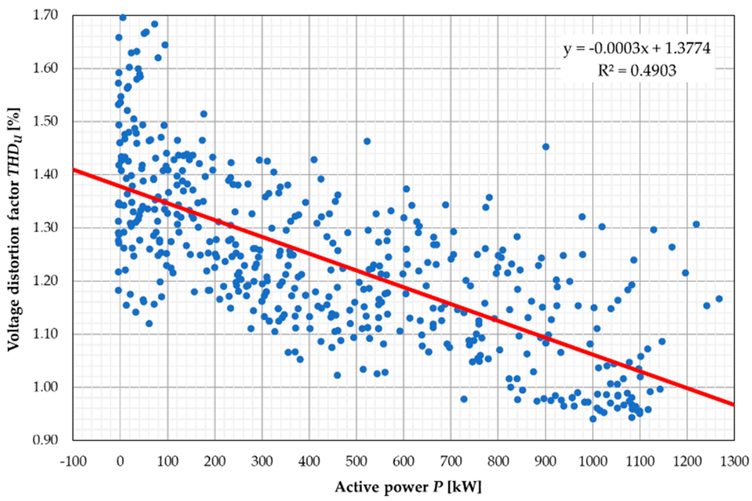

Figure 15. Dependence of the voltage distortion factor THD_U on the active power P generated at the connection point of the photovoltaic farm under study.

The distribution of values presented in Figure 15 clearly shows an inversely proportional relationship between the voltage distortion factor THD_U and the power generated via the photovoltaic farm. This means that the devices installed in the photovoltaic installation do not have a negative impact in terms of voltage distortion. The increase in active power generation in the source reduces the voltage distortion from the sinusoidal waveform occurring in the power grid. It can also be observed that this is an approximately rectilinear relationship.

5. Discussion and Summary

Summarizing the results of statistical calculations and in situ measurements, the following conclusions can be drawn regarding the analyzed factors describing the quality of electricity occurring at the power plant connection point.

Power generation in a photovoltaic power plant causes an increase in voltage. According to simulation analyses, these changes resulted in a voltage deviation of approximately 6% of the rated voltage at maximum generation. The voltage deviation values recorded in field measurements ranged from 3.1% to 6.51%. The values obtained analytically and experimentally are, therefore, very close to each other. This confirms the conclusions noted by other authors [47,51,53] that a photovoltaic power plant significantly affects the voltage stability in the power grid. However, this impact depends on the power of the power plant and the place of its connection. Therefore, it is very important to perform technical expertise before issuing a permit for the construction of an energy source to determine the possibilities of connecting a power plant at a given point in the power system.

As the power generated in a photovoltaic power plant increases, the value of the zero-sequence voltage asymmetry factor decreases. According to simulation calculations, this change for the analyzed power plant ranged from 2.81 to 1.32%. The values obtained from field tests, after discarding values outside the main set, ranged from 1.39 to 1.73%.

The upper value of the zero-sequence asymmetry factor, in the absence of generation, in real conditions was more than 1% higher than the simulation results. Nevertheless, the k_{U0} values at full generation were similar in both cases.

The values of the negative-sequence voltage asymmetry factor are the highest when there is no generation in the photovoltaic installation. However, in the case of analytically determined values, the k_{U2} factor variability curve takes the shape of a parabolic curve, with the minimum occurring at 75% of the rated power of the plant. In the case of analytically determined relationships, the increase in the value of the negative-sequence voltage asymmetry factor at generation close to the maximum is not very noticeable. However, it should be emphasized that during field measurements, due to the weather conditions occurring during them, the rated power of the power plant could not be achieved, but only 72% P_n. It can, therefore, be concluded that in the power ranges analyzed in both cases, the patterns of variability of the asymmetry factors are analogous. The ranges of the recorded values of the k_{U2} factor are also comparable, which in both cases range from approximately 0.2 to 0.5%. The analytical values obtained are slightly lower than those measured in the real system.

The last parameter analyzed was the voltage distortion factor THD_U. In this case, a decrease in the *THD* factor was also noticed with the increase in power generated at the source. According to analytical calculations, this change was close to 20%. The recorded values of this factor in the real system decreased by almost 60%. Compared to simulation, higher values of the voltage distortion factor THD_U without generation were recorded, and lower ones at maximum generation. In this case, neither the results of simulation tests nor field tests performed in a medium-voltage system confirmed the relationships shown in [46–48] for low-voltage power systems. According to the research carried out by the authors, power generation in a photovoltaic power plant clearly reduces the voltage distortion factor in the 15 kV network, while, according to the literature [46–48], in low-voltage networks with the increase in power generated in the photovoltaic installation the value THD_U coefficient increases. This is a very important difference in the context of network stability and the quality of electricity transmitted through it.

By comparing the values of the analyzed electricity quality indicators obtained by the authors as a result of simulation and field tests, all analyzed indicators meet the requirements applicable in Europe and around the world. The value of the THD_U coefficient does not exceed 2% in any analyzed case, with the required (depending on the country) 5% or 8%. The same happens with the values of voltage deviations and asymmetry. The voltage deviation caused by the operation of the analyzed photovoltaic power plant did not exceed 6.5% of the rated voltage, with the 10% required by law. The reverse voltage unbalance factor recorded by the authors was also significantly lower than the values required in global regulations (2% or 1%) and in no case exceeded 0.65%.

To sum up, the impact of a photovoltaic power plant on the power grid can be divided into two groups: positive and negative. The negative impact of the operation of a photovoltaic farm includes primarily an increase in the voltage value at the farm connection point. This is a well-known phenomenon that distribution network operators and connected customers struggle with every day. It often happens that the voltage value exceeds 110% of the rated network voltage, which causes the protection automation to exclude individual inverters from production. It is often necessary to use various technical solutions to limit the range of voltage changes. In other cases, the operation of the photovoltaic farm improves parameters describing the quality of electricity supply, such as the voltage asymmetry factors (zero- and negative-sequence) or the voltage distortion factors. The determined values of these factors decrease with the increase in the power generated via the farm, even though at no time during the tests did they exceed the permissible values specified in the currently applicable regulations.

Author Contributions: Conceptualization, G.H. and Z.S.; methodology, G.H.; software, G.H.; validation, G.H., Z.S. and A.F.; formal analysis, A.F. and Z.S.; investigation, G.H.; resources, G.H. and Z.S.; data curation, G.H., A.F. and Z.S.; writing—original draft preparation, Z.S. and W.W.; writing—review and editing, A.F. and W.W.; visualization, G.H. and W.W.; supervision, W.W.; project administration, G.H. and Z.S.; funding acquisition, W.W. All authors have read and agreed to the published version of the manuscript.

Funding: The work was supported by scientific work WZ/WE-IA/7/2023 conducted in the Department of Electrotechnics, Power Electronics, and Electrical Power Engineering at Bialystok University of Technology.

Data Availability Statement: Data are contained within the article.

Conflicts of Interest: The authors declare no conflicts of interest.

References

1. Villa-Ávila, E.; Arévalo, P.; Aguado, R.; Ochoa-Correa, D.; Iñiguez-Morán, V.; Jurado, F.; Tostado-Véliz, M. Enhancing Energy Power Quality in Low-Voltage Networks Integrating Renewable Energy Generation: A Case Study in a Microgrid Laboratory. *Energies* **2023**, *16*, 5386. [CrossRef]
2. Wu, J.-C.; Jou, H.-L.; Chang, C.-H. Power Conversion Interface for a Small-Capacity Photovoltaic Power Generation System. *Energies* **2023**, *16*, 1097. [CrossRef]
3. Chen, Z.; Wang, X.; Kang, S. Effect of the Coupled Pitch–Yaw Motion on the Unsteady Aerodynamic Performance and Structural Response of a Floating Offshore Wind Turbine. *Processes* **2021**, *9*, 290. [CrossRef]
4. Skibko, Z.; Hołdyński, G.; Borusiewicz, A. Impact of Wind Power Plant Operation on Voltage Quality Parameters—Example from Poland. *Energies* **2022**, *15*, 5573. [CrossRef]
5. *EN 50160:2022*; Voltage Characteristics of Electricity Supplied by Public Electricity Networks. CENELEC: Brussels, Belgium, 2022. Available online: https://standards.cencenelec.eu/dyn/www/f?p=CENELEC:110:::::FSP_PROJECT,FSP_ORG_ID:71003,1258595&cs=177F89A233554A3CA651BC5AAA21C3EB3 (accessed on 12 January 2024).
6. The Internet System of Legal Acts—ISAP Regulation of the Minister of Climate and Environment of March 22, 2023 on Detailed Conditions for the Operation of the Power System. Available online: https://isap.sejm.gov.pl/isap.nsf/DocDetails.xsp?id=WDU20230000819 (accessed on 12 January 2024).
7. Angelo, B. *Handbook of Power Quality*; Baggini, A., Ed.; Wiley: Hoboken, NJ, USA, 2008; ISBN 9780470065617.
8. Singh, B.; Chandra, A.; Al-Haddad, K. (Eds.) *Power Quality Problems and Mitigation Techniques*; Wiley: Hoboken, NJ, USA, 2015; ISBN 9781118922057.
9. Tang, L.; Han, Y.; Yang, P.; Wang, C.; Zalhaf, A.S. A Review of Voltage Sag Control Measures and Equipment in Power Systems. *Energy Rep.* **2022**, *8*, 207–216. [CrossRef]
10. Gandoman, F.H.; Ahmadi, A.; Sharaf, A.M.; Siano, P.; Pou, J.; Hredzak, B.; Agelidis, V.G. Review of FACTS Technologies and Applications for Power Quality in Smart Grids with Renewable Energy Systems. *Renew. Sustain. Energy Rev.* **2018**, *82*, 502–514. [CrossRef]
11. Zajkowski, K.; Duer, S. Decomposition of the Voltages in a Three-Phase Asymmetrical Circuit with a Non-Sinusoidal Voltage Source. *Energies* **2023**, *16*, 7616. [CrossRef]
12. Machowski, J.; Lubosny, Z.; Bialek, J.W.; Bumby, J.R.; James, R. *Power System Dynamics: Stability and Control*; John Wiley & Sons: Hoboken, NJ, USA, 2020; p. 855.
13. Mroz, M.; Chmielowiec, K.; Hanzelka, Z. Voltage Fluctuations in Networks with Distributed Power Sources. In Proceedings of the 2012 IEEE 15th International Conference on Harmonics and Quality of Power, Hong Kong, China, 17–20 June 2012; pp. 920–925.
14. Nempu, P.B.; Sabhahit, J.N.; Gaonkar, D.N.; Rao, V.S. Novel Power Smoothing Technique for a Hybrid AC-DC Microgrid Operating with Multiple Alternative Energy Sources. *Adv. Electr. Comput. Eng.* **2021**, *21*, 99–106. [CrossRef]
15. Ma, W.; Wang, W.; Wu, X.; Hu, R.; Tang, F.; Zhang, W. Control Strategy of a Hybrid Energy Storage System to Smooth Photovoltaic Power Fluctuations Considering Photovoltaic Output Power Curtailment. *Sustainability* **2019**, *11*, 1324. [CrossRef]
16. Krishan, O.; Suhag, S. A Novel Control Strategy for a Hybrid Energy Storage System in a Grid-independent Hybrid Renewable Energy System. *Int. Trans. Electr. Energy Syst.* **2020**, *30*, e12262. [CrossRef]
17. Chong, L.W.; Wong, Y.W.; Rajkumar, R.K.; Isa, D. An Optimal Control Strategy for Standalone PV System with Battery-Supercapacitor Hybrid Energy Storage System. *J. Power Sources* **2016**, *331*, 553–565. [CrossRef]
18. Wu, T.; Yu, W.; Guo, L. A Study on Use of Hybrid Energy Storage System Along with Variable Filter Time Constant to Smooth DC Power Fluctuation in Microgrid. *IEEE Access* **2019**, *7*, 175377–175385. [CrossRef]
19. Hołdyński, G.; Skibko, Z.; Borusiewicz, A. Analysis of the Influence of Load on the Value of Zero-Voltage Asymmetry in Medium-Voltage Networks Operating with Renewable Energy Sources. *Energies* **2023**, *16*, 580. [CrossRef]
20. Kim, Y.-J. Development and Analysis of a Sensitivity Matrix of a Three-Phase Voltage Unbalance Factor. *IEEE Trans. Power Syst.* **2018**, *33*, 3192–3195. [CrossRef]
21. Neukirchner, L.; Görbe, P.; Magyar, A. Voltage Unbalance Reduction in the Domestic Distribution Area Using Asymmetric Inverters. *J. Clean Prod.* **2017**, *142*, 1710–1720. [CrossRef]
22. Al-Shetwi, A.Q.; Hannan, M.A.; Jern, K.P.; Alkahtani, A.A.; PG Abas, A.E. Power Quality Assessment of Grid-Connected PV System in Compliance with the Recent Integration Requirements. *Electronics* **2020**, *9*, 366. [CrossRef]

23. Moller, F.; Meyer, J. Survey of Voltage Unbalance and Unbalanced Power in German Public LV Networks. In Proceedings of the 2022 20th International Conference on Harmonics & Quality of Power (ICHQP), Naples, Italy, 29 May–1 June 2022; pp. 1–6.
24. Paranavithana, P.; Perera, S.; Koch, R.; Emin, Z. Global Voltage Unbalance in MV Networks Due to Line Asymmetries. *IEEE Trans. Power Deliv.* **2009**, *24*, 2353–2360. [CrossRef]
25. Püvi, V.; Lehtonen, M. Convex Model for Estimation of Single-Phase Photovoltaic Impact on Existing Voltage Unbalance in Distribution Networks. *Appl. Sci.* **2020**, *10*, 8884. [CrossRef]
26. Schwanz, D.; Moller, F.; Ronnberg, S.K.; Meyer, J.; Bollen, M.H.J. Stochastic Assessment of Voltage Unbalance Due to Single-Phase-Connected Solar Power. *IEEE Trans. Power Deliv.* **2017**, *32*, 852–861. [CrossRef]
27. Kuboń, M.; Skibko, Z.; Tabor, S.; Malaga-Toboła, U.; Borusiewicz, A.; Romaniuk, W.; Zarajczyk, J.; Neuberger, P. Analysis of Voltage Distortions in the Power Grid Arising from Agricultural Biogas Plant Operation. *Energies* **2023**, *16*, 6189. [CrossRef]
28. Burg, V.; Bowman, G.; Haubensak, M.; Baier, U.; Thees, O. Valorization of an Untapped Resource: Energy and Greenhouse Gas Emissions Benefits of Converting Manure to Biogas through Anaerobic Digestion. *Resour. Conserv. Recycl.* **2018**, *136*, 53–62. [CrossRef]
29. Roy, R.B.; Alahakoon, S.; Arachchillage, S.J. Grid Impacts of Uncoordinated Fast Charging of Electric Ferry. *Batteries* **2021**, *7*, 13. [CrossRef]
30. Nour, M.; Chaves-Ávila, J.P.; Magdy, G.; Sánchez-Miralles, Á. Review of Positive and Negative Impacts of Electric Vehicles Charging on Electric Power Systems. *Energies* **2020**, *13*, 4675. [CrossRef]
31. Rodríguez-Pajarón, P.; Hernández, A.; Milanović, J.V. Probabilistic Assessment of the Impact of Electric Vehicles and Nonlinear Loads on Power Quality in Residential Networks. *Int. J. Electr. Power Energy Syst.* **2021**, *129*, 106807. [CrossRef]
32. Held, L.; Mueller, F.; Steinle, S.; Barakat, M.; Suriyah, M.R.; Leibfried, T. An Optimal Power Flow Algorithm for the Simulation of Energy Storage Systems in Unbalanced Three-Phase Distribution Grids. *Energies* **2021**, *14*, 1623. [CrossRef]
33. Weckx, S.; Driesen, J. Load Balancing With EV Chargers and PV Inverters in Unbalanced Distribution Grids. *IEEE Trans. Sustain. Energy* **2015**, *6*, 635–643. [CrossRef]
34. Figueira, H.H.; Hey, H.L.; Schuch, L.; Rech, C.; Michels, L. Brazilian Grid-Connected Photovoltaic Inverters Standards: A Comparison with IEC and IEEE. In Proceedings of the 2015 IEEE 24th International Symposium on Industrial Electronics (ISIE), Buzios, Brazil, 3–5 June 2015; pp. 1104–1109.
35. ANRE Anre.Ro—Autoritatea Națională de Reglementare În Domeniul Energiei. RAE–Regulatory Authority for Energy. Technical Transmission Grid Code of the Romanian Power System. Available online: https://anre.ro/ (accessed on 21 January 2024).
36. Petružela, M.; Blažek, V.; Vysocký, J. Analysis of Appliance Impact on Total Harmonic Distortion in Off-Grid System. In *AETA 2018-Recent Advances in Electrical Engineering and Related Sciences: Theory and Application*; Springer International Publishing: Berlin/Heidelberg, Germany, 2020; pp. 844–849.
37. Aboutaleb, A.M.; Desmet, J.; Knockaert, J. Impact of Grid-Connected Inverter Parameters on the Supraharmonic Emissions in Distributed Power Generation Systems. *Machines* **2023**, *11*, 1014. [CrossRef]
38. Sun, Y.; Li, S.; Xu, Q.; Xie, X.; Jin, Z.; Shi, F.; Zhang, H. Harmonic Contribution Evaluation Based on the Distribution-Level PMUs. *IEEE Trans. Power Deliv.* **2021**, *36*, 909–919. [CrossRef]
39. Gao, B.; Wang, Y.; Xu, W. An Improved Model of Voltage Source Converters for Power System Harmonic Studies. *IEEE Trans. Power Deliv.* **2022**, *37*, 3051–3061. [CrossRef]
40. Torquato, R.; Hax, G.R.T.; Freitas, W.; Nassif, A. Impact Assessment of High-Frequency Distortions Produced by PV Inverters. *IEEE Trans. Power Deliv.* **2021**, *36*, 2978–2987. [CrossRef]
41. Tarafdar Hagh, M.; Khalili, T. A Review of Fault Ride through of PV and Wind Renewable Energies in Grid Codes. *Int. J. Energy Res.* **2019**, *43*, 1342–1356. [CrossRef]
42. Lee, J.H.; Ho Yoon, Y.; Kim, J.M. Analysis of IEC 61727 Photovoltaic (PV) Systems Characteristics of the Utility Interface. *Int. J. Internet Broadcast. Commun.* **2015**, *7*, 90–95. [CrossRef]
43. IEEE SA Board of Governors IEEE SA—IEEE 1547a-2014. Available online: https://standards.ieee.org/ieee/1547a/5531/ (accessed on 21 January 2024).
44. *IEEE Std 519-1992*; IEEE Recommended Practices and Requirements for Harmonic Control in Electrical Power Systems IEEE Industry Applications Society/Power Engineering Society. The Institute of Electrical and Electronics Engineers, Inc.: Piscataway, NJ, USA, 1993.
45. Green System Operator ECM–Energy Commission Malaysia. Grid Code for Peninsular Malaysia. Available online: https://www.gso.org.my/ (accessed on 21 January 2024).
46. Kopicka, M.; Ptacek, M.; Toman, P. Analysis of the Power Quality and the Impact of Photovoltaic Power Plant Operation on Low-Voltage Distribution Network. In Proceedings of the 2014 Electric Power Quality and Supply Reliability Conference (PQ), Rakvere, Estonia, 11–13 June 2014; pp. 99–102.
47. Abdul Kadir, A.F.; Khatib, T.; Elmenreich, W. Integrating Photovoltaic Systems in Power System: Power Quality Impacts and Optimal Planning Challenges. *Int. J. Photoenergy* **2014**, *2014*, 321826. [CrossRef]
48. Amirullah; Penangsang, O.; Soeprijanto, A. Effect of Installation of Photovoltaic (PV) Generation to Power Quality in Industrial and Residential Customers Distribution Network. In Proceedings of the 2015 International Seminar on Intelligent Technology and Its Applications (ISITIA), Surabaya, Indonesia, 20–21 May 2015; pp. 193–200.

49. Barker, P.P.; De Mello, R.W. Determining the Impact of Distributed Generation on Power Systems. I. Radial Distribution Systems. In Proceedings of the 2000 Power Engineering Society Summer Meeting (Cat. No.00CH37134), Seattle, WA, USA, 16–20 July 2000; pp. 1645–1656.
50. Kim, S.-K.; Jeon, J.-H.; Cho, C.-H.; Kim, E.-S.; Ahn, J.-B. Modeling and Simulation of a Grid-Connected PV Generation System for Electromagnetic Transient Analysis. *Sol. Energy* **2009**, *83*, 664–678. [CrossRef]
51. Elshahed, M.A. Assessment of Sudden Voltage Changes and Flickering for a Grid-Connected Photovoltaic Plant. *Int. J. Renew. Energy Res.* **2016**, *6*, 1328–1335. [CrossRef]
52. Salah Saidi, A.; Ben-Kilani, K.; Elleuch, M. Impact of Large Scale Photovoltaic Generation on Voltage Stability in Distribution Networks. *Eur. J. Electr. Eng.* **2016**, *18*, 117–138. [CrossRef]
53. Till, J.; You, S.; Liu, Y.; Du, P. Impact of High PV Penetration on Voltage Stability. In Proceedings of the 2020 IEEE/PES Transmission and Distribution Conference and Exposition (T&D), Chicago, IL, USA, 12–15 October 2020; pp. 1–5.
54. Hossain, E.; Tur, M.R.; Padmanaban, S.; Ay, S.; Khan, I. Analysis and Mitigation of Power Quality Issues in Distributed Generation Systems Using Custom Power Devices. *IEEE Access* **2018**, *6*, 16816–16833. [CrossRef]

Disclaimer/Publisher's Note: The statements, opinions and data contained in all publications are solely those of the individual author(s) and contributor(s) and not of MDPI and/or the editor(s). MDPI and/or the editor(s) disclaim responsibility for any injury to people or property resulting from any ideas, methods, instructions or products referred to in the content.